Pakistan Veterinary Journal

ISSN: 0253-8318 (PRINT), 2074-7764 (ONLINE)
DOI: 10.29261/pakvetj/2026.103

RESEARCH ARTICLE

Multi-Omics Uncovers Formononetin's Protection Against Antibiotic-Induced Liver Injury Via Microbiota-Metabolite-Transcriptome Coordination

Xue Zhang[1,4,†], Xinyi Wang[3,†], Jiatong Sui[1,†], Eman A Al-Shahari[6], Layla A. Almutairi [7], Yue Yu[3], Shouhai Chen[3], Wenqing Jiang[3], Yan Luo[1], Yunyue Hu[1], Ning Wang[1], Xiaolong Gu[1], Jian Sun[1], Ning Li[5,*], Weibing Bai[1,*] and Weijie Qu[1,*]

[1]College of Veterinary Medicine, Yunnan Agricultural University, Kunming 650201, Yunnan Province, China; [2]College of Basic Medicine, Inner Mongolia Medical University, Chilechuan Dairy Economic Development Zone, Hohhot 010110, Inner Mongolia Autonomous Region, China; [3]College of Veterinary Medicine, Nanjing Agricultural University, Nanjing 210095, Jiangsu Province, China; [4]College of Veterinary Science and Technology, Yunnan Agricultural University, Kunming 650201, Yunnan Province, China; [5]College of traditional Chinese medicine, Yunnan University of Chinese Medicine, Kunming 650500, China; [6]Health Specialties, Basic Sciences and Their Applications Unit, Applied College at Muhayil Asir, King Khalid University, Abha, Saudi Arabia.; [7]Department of Biology, College of Science, Princess Nourah bint Abdulrahman University, P.O. Box 84428, Riyadh 11671, Saudi Arabia
[†]These authors contributed equally to this article
*Corresponding author: mailtolining@gmail.com; wjqu@ynau.edu.cn; 360536885@qq.com

ARTICLE HISTORY (26-356)

Received: March 27, 2026
Revised: May 14, 2026
Accepted: May 16, 2026
Published online: May 19, 2026

Key words:
Ferroptosis
Gut-liver axis
Isoflavone formononetin
Microbiota-metabolome crosstalk
Multi-omics integration
TET-mediated hepatic injury

ABSTRACT

Tetracycline antibiotics (TETs) are widely used in veterinary practice but can induce acute hepatotoxicity upon overdose, compromising animal health and productive performance. This study evaluated whether the natural isoflavone formononetin (FMN) can alleviate TET-induced liver injury in animals via coordinated regulation of the gut microbiota–metabolite–transcriptome axis. Using network toxicology and pharmacology, we predicted key targets and pathways involved. A mouse model of of acute, overdose-induced TET-associated liver injury (150 mg/kg, once daily for 3 days) was treated with FMN (50 or 100 mg/kg) for 14 days. Multi-omics analyses revealed that FMN attenuated hepatic steatosis, reduced ALT/AST levels, enhanced gut microbial diversity (enriched *Limosilactobacillus*) and restored intestinal barrier integrity. Mechanistically, FMN activated the Nrf2/HO-1 antioxidant pathway, modulated PPARα/CYP2E1-dependent lipid metabolism, and may be associated with ferroptosis inhibition. In summary, FMN exerts multi-target hepatoprotective effects by coordinately regulating gut microbiota homeostasis, alleviating oxidative stress and remodeling hepatic metabolic networks, thereby providing a preliminary basis for further evaluation of formononetin for antibiotic-associated liver injury in veterinary settings.

To Cite This Article: Zhang X, Wang X, Sui J, Al-Shahari EA, Almutairi LA, Yu Y, Chen S, Jiang W, Luo Y, Hu Y, Wang N, Gu X, Sun J, Li N, Bai W and Qu W, 2026. Multi-omics uncovers formononetin's protection against antibiotic-induced liver injury via microbiota-metabolite-transcriptome coordination. Pak Vet J, 46(5): 1152-1166. http://dx.doi.org/10.29261/pakvetj/2026.103

INTRODUCTION

Tetracyclines (TETs) are broad-spectrum antibiotics widely used in both human medicine and animal husbandry due to their cost-effectiveness and efficacy against a variety of bacterial pathogens (Li *et al.*, 2024). However, their extensive and often indiscriminate application has led to concerning levels of environmental contamination, with TET residues frequently detected in soil, water systems, and animal-derived food products such as meat, milk, and eggs (Tóth *et al.*, 2013; Liu *et al.*, 2025). Beyond environmental impact, TETs pose significant health risks, particularly drug-induced liver injury (DILI). Recent surveillance data from the United States indicate that TETs are responsible for 17.3% of all antibiotic-associated DILI cases, with a striking 82% of these presenting as severe microvesicular steatosis (Kennedy *et al.*, 2021). Notably, food-producing animals and populations with long-term exposure to veterinary antibiotics face a 2.1-fold higher risk of liver injury compared to the general population (Wei *et al.*, 2022). Clinically, tetracycline itself has been documented to

cause drug-induced liver injury (Silva *et al.*, 2023), and its derivative minocycline can induce acute hepatitis and even liver failure (Wang *et al.*, 2024a). Thus, the 3-day tetracycline regimen used in the present study models a clinically relevant scenario of acute hepatotoxicity resulting from tetracycline overdose or short-term exposure.

Upon entering the body via the food chain, TETs preferentially accumulate in the liver and induce damage through three main pathways: (1) inhibition of mitochondrial β-oxidation, leading to microvesicular steatosis (Shao *et al.*, 2025); (2) disruption of the gut microbiota-liver axis, exacerbating oxidative stress (Vitale *et al.*, 2023); and (3) induction of hepatocyte apoptosis, clinically manifested as rapid elevation of ALT/AST accompanied by jaundice (Kennedy *et al.*, 2021). In veterinary clinical observations, TET-induced fatty liver presents as hepatic microvesicular steatosis, which falls under the category of secondary non-alcoholic fatty liver disease. Compared to macrovesicular steatosis, microvesicular steatosis has a poorer prognosis and higher risk of progression to steatohepatitis.

Formononetin (FMN), an isoflavonoid compound abundantly present in various Chinese medicinal herbs such as *Spatholobus suberectus*, *Sophora flavescens* and *Astragalus membranaceus* (Zhang *et al.*, 2018), exhibits low toxicity and minimal side effects (Tay *et al.*, 2019; Yang *et al.*, 2022). Studies have demonstrated that FMN can enhance the richness and diversity of gut microbiota in mice, modify microbial composition by promoting beneficial bacteria, and function as a potential prebiotic to effectively regulate host metabolism, reduce systemic inflammation, and improve gut microbiota structure (Naudhani *et al.*, 2021). Furthermore, studies have demonstrated that FMN exhibits notable pharmacological activities such as anti-inflammatory, antioxidant, and immunomodulatory effects, showing promise in treating NAFLD, drug-induced liver injury, and cholestatic liver disease (Wang *et al.*, 2019; Liao *et al.*, 2024). We hypothesize that FMN may alleviate TET-induced DILI, but its specific effects and underlying mechanisms in this context remain poorly understood.

Toxicology and network pharmacology—these two powerful in-silico methods are widely used to predict compound toxicity and elucidate the multi-target mechanisms of natural products. They facilitate the construction of systematic mechanistic hypotheses and provide clear directions for subsequent experimental validation, thereby significantly enhancing the efficiency and focus of research.

In this study, we combined computational toxicology and network pharmacology prediction with a multi-omics approach—integrating 16S rRNA sequencing, transcriptomics, and metabolomics—alongside biochemical and histopathological assessments to systematically evaluate the protective effects of FMN in a mouse model of TET-induced DILI. By first predicting key targets and pathways through bioinformatic analyses, we established a mechanistic foundation for experimental validation. Our integrated strategy not only clarifies FMN's protective mechanisms at the molecular and metabolic levels but also provides novel insights into the role of natural isoflavones in alleviating antibiotic-associated liver damage. These findings may provide a basis for future evaluation of formononetin in veterinary applications.

MATERIALS AND METHODS

Screening of FMN targets: The SMILES notation of FMN was obtained from PubChem. Potential therapeutic targets in Homo sapiens were predicted using SwissTargetPrediction and ChEMBL databases, and the results were consolidated into a candidate target library.

PPI network and Venn analysis: Common targets intersecting DILI-related and tetracycline (TET)-induced hepatotoxicity sets overlapped with predicted FMN targets. The overlapping genes were imported into STRING (version 11.5) to construct a PPI network with a minimum interaction score of 0.900. KEGG pathway analysis was performed using DAVID ($P<0.05$). Venn diagrams were constructed using the Bioinformatics online platform.

Experimental animals and protocol: Male ICR mice (4 weeks old, 18–22g) were purchased from Yangzhou University. After 7 days of acclimatization, all animals were housed under controlled conditions (22 ± 2°C, 12 h light/dark cycle) with free access to standard chow and water. mice were randomly divided into four groups: NC (0.5% carboxymethyl cellulose sodium, CMC-Na), Model (0.5% CMC-Na), FMNL (FMN low-dose, 50 mg/kg), and FMNH (FMN high-dose, 100mg/kg); FMN (purity ≥98%) was purchased from Macklin and dissolved in 0.5% CMC-Na. After 14 days of treatment, the DILI model was induced by intraperitoneal injection of tetracycline (150mg/kg) from day 12 to 14, while the control group received sterile saline. No other hepatotoxic agents were used, confirming that liver injury is attributable to tetracycline. On day 15, blood, liver, colon, and fecal samples were collected.

Biochemical assays: Serum was isolated by centrifugation. Biochemical parameters were measured according to the manufacturer's instructions. Liver tissue was homogenized in ice-cold PBS (1:9 w/v), and the supernatant was used for biochemical assays following kit protocols.

Histopathological analysis: Freshly collected liver and colon tissues were fixed in 4% paraformaldehyde for 24h, followed by H&E staining, Oil Red O staining, and immunohistochemical analysis.

RT-qPCR analysis: Total RNA was extracted using an RNA Extraction Kit. RNA concentration and purity were measured by NanoDrop spectrophotometry. First-strand cDNA was synthesized using HiScript II Q RT SuperMix. Quantitative PCR was performed using ChamQ SYBR qPCR Master Mix on a BIO-RAD system. B-actin was used as the reference gene, and relative mRNA expression was calculated using the $2^{-\Delta\Delta Ct}$ method (Table 1).

16S rRNA sequencing: Fecal DNA was extracted using a DNA extraction kit. The V3-V4 hypervariable regions of

16S rRNA genes were amplified and sequenced on the NovaSeq platform. Raw data were processed using the QIIME2 pipeline, including DADA2 denoising to generate ASVs and taxonomic classification using the SILVA v138 database. A-diversity and β-diversity analyses were performed, and functional pathways were predicted using PICRUSt2. Differential abundance of taxa was assessed with FDR correction (q<0.05).

Table 1: Primer information

Primer Name	Primer Sequences(5'to3')
β-actin-F	CCTGTACGCCAACACAGTGC
β-actin-R	ATACTCCTGCTTGCTGATCC
PPARα-F	CTTTACATCAGTGTTTCCGTCAG
PPARα-R	TCAAATTGCCACCGTTCTT
AOX-F	ACTGCGTGGGCCATCTTGTCTG
AOX-R	TTCCTGGCCGCCTATGTGTAT
Cyp2E1-F	GGCGCATCGTGGTCCTGCAT
Cyp2E1-R	GGCTGGCCTTTGGTCTTTTTGAGC
Cyp1A2-F	AGGGACACCTCACTGAATGGC
Cyp1A2-R	GGGTCTTTCCACTGCTTCTCATC
FAS-F	TCATTTGTGGCCTTCTCCTCTGTAA
FAS-R	CTTCCACACCCATGAGCGAGTCCAGGCCGA
Nrf2-F	TAGATGACCATGAGTCGCTTGC
Nrf2-R	GCCAAACTTGCTCCATGTCC
HO-1-F	GATAGAGCGCAACAAGCAGAA
HO-1-R	CAGTGAGGCCCATACCAGAAG
Prdx3-F	TTCCCACTTCAGTCATCTTGCC
Prdx3-R	ATGCCAGCACTTTCCAACAG

Fecal SCFA analysis: Short-chain (C2-C6) and medium-chain (C7-C12) fatty acids were quantified by GC-MS/MS. Fecal samples were homogenized in 0.5% phosphoric acid and extracted with methyl tert-butyl ether containing internal standards. Separation was performed on a DB-FFAP capillary column with detection in multiple reaction monitoring mode. Statistical comparisons of SCFA levels were performed using one-way ANOVA with FDR correction (Benjamini–Hochberg, q<0.05).

Liver transcriptomics: High-quality RNA (RIN>8) was used for library preparation with the NEBNext® Ultra™ RNA Kit. Sequencing on an Illumina platform generated 150 bp paired-end reads. Raw reads were trimmed (Fastp), aligned to mm10 (HISAT2), and quantified (featureCounts). Differential expression analysis used DESeq2 (|log2FC|>1, FDR<0.05). Functional enrichment of KEGG pathways and GO terms used clusterProfiler.

Liver metabolomics: Liver tissue samples (100mg) were extracted with methanol/water (80:20). Chromatographic separation was performed on a C18 column with a 10-minute gradient elution. Mass spectrometric detection was performed using high-resolution Q-TOF instrumentation with electrospray ionization. Compound identification integrated precursor mass, fragmentation patterns, and retention time alignment against curated databases. Multivariate pattern recognition (VIP>1) and univariate significance testing (adjusted P<0.05, ≥2-fold change) were applied, followed by metabolic pathway mapping.

Multi-omics integration analysis. Correlation between gut microbiota (genus level), liver metabolome, and liver transcriptome was assessed using Spearman's rank correlation coefficient. Significant correlations were defined as $|r| > 0.5$ and adjusted P<0.05 (FDR). Co-enriched KEGG pathways between differential metabolites and differential genes were identified using cluster Profiler (P<0.05). Fecal short-chain fatty acids were not included in this integration due to lack of significant differences among groups. All integration analyses were performed in R (version 4.2).

Statistical analysis: Quantitative data are expressed as mean ± SEM. Statistical comparisons were performed in GraphPad Prism 10 using one-way ANOVA with Tukey's post-hoc test (*P<0.01, **P<0.001). For multi-omics data (transcriptomics, metabolomics, 16S rRNA), false discovery rate (FDR) correction (Benjamini–Hochberg, $q < 0.05$) was applied to account for multiple comparisons, as detailed in the respective method sections.

RESULTS

Network pharmacology and computational toxicology elucidate FMN's protective mechanisms against TET-induced liver injury: We obtained the 2D structures and SMILES numbers of TET and FMN from PubChem and further visualized the structures using ChemDraw (Fig. 1A). Our computational toxicology analysis predicted Tetracycline (TET) to be hepatotoxic (Toxicity Class 4; DILI probability: 0.58) (Fig. 1A). Through an integrative network pharmacology approach (Fig. 1B-D), we identified 39 common targets at the intersection of drug-induced liver injury (DILI), TET, and Formononetin (FMN), suggesting these as the potential core mechanisms for FMN's protective effects (Fig. 1B). Functional enrichment analysis of these 39 targets revealed significant involvement in key pathways including the PI3K-Akt, cGMP-PKG, and JAK-STAT signaling pathways (Fig. 1C). Furthermore, protein-protein interaction (PPI) network analysis pinpointed several high-degree hub genes, such as *Bcl2*, *Egfr*, *Ptgs2*, *Esr1*, *Gsk3b*, *Mapk1*, and *Kit*, which are predicted to play central roles in the therapeutic action of FMN against TET-induced liver injury (Fig. 1D).

FMN attenuates TET-induced hepatic damage: The MODEL group showed significantly increased liver index (P<0.001, Fig. 2B) and serum AST levels (P<0.01, Fig. 2C), with ALT demonstrating an upward trend (Fig. 2D). Histological examination revealed severe steatosis and necrosis (Fig. 2E), along with significantly expanded lipid droplet area (P<0.001, Fig. 2F), elevated TC and TG levels (both P<0.001, Fig. 2G-H), and decreased HDL/LDL ratio (P<0.05, Fig. 2I). FMN administration significantly reversed these alterations (liver index/AST: P<0.05; lipid parameters: P<0.001, Fig. 2B-I). At the molecular level, while FAS expression remained unchanged (Fig. 2J), the downregulation of β-oxidation genes (*PPARα, AOX, CYP2E1*: all P<0.001, Fig. 2K-M) was completely restored by FMN treatment.

FMN alleviates TET-induced oxidative stress: TET exposure significantly impaired the antioxidant defense system, evidenced by elevated serum SOD inhibition (P<0.001, Fig. 3A), suppressed hepatic SOD activity (P<0.01, Fig. 3B), and reduced serum GSH levels (P<0.01, Fig. 3C). Molecular analyses revealed

downregulation of key antioxidant genes, including *Nrf2*, *HO-1*, *Prdx3*, *and Cyp1a2* (all P<0.001, Fig. 3D-G). FMNH treatment effectively counteracted these changes, restoring oxidative stress markers to near-normal levels, which demonstrates its potent antioxidative properties against TET-induced hepatotoxicity.

FMN ameliorates TET-induced colonic barrier damage and gut microbiota dysbiosis: We evaluated TET-induced intestinal barrier damage and FMN's restorative effects through colonic histology, tight junction protein expression, and serum LPS levels. H&E staining revealed villus detachment in the TET-treated model group (Fig. 4A), with significantly reduced Occludin expression (P<0.001) and elevated serum LPS (P<0.001). FMN treatment dose-dependently reversed these changes (Fig. 4A-D), demonstrating its ability to repair TET-induced intestinal barrier disruption.

16S rRNA sequencing analysis revealed that PCA analysis showed a clear distinction between the blank control group and the TET-treated group (Fig. 5A). Venn diagram analysis indicated that the model had the lowest number of OTUs, while the FMNH group exhibited an © count intermediate between the model and NC groups (Fig. 5B). TET significantly reduced the α-diversity of the gut microbiota (Faith's PD), as well as Chao, Shannon, and Simpson indices, and FMNH reversed this effect (Fig. 5C). β-diversity (unweighted UniFrac) analysis demonstrated that the NC and FMN groups had richer microbiota diversity compared to the model group (Fig. 5D). LefSe and random forest analyses identified key bacterial phyla: *Verrucomicrobiota*, *Deferribacterota*, *Desulfobacterota_1*, *Firmicutes_B_370539*, *Cyanobacteria*, *Acidobacteriota*, and *Patescibacteria_A_473307*, which were sensitive to TET and modulated by FMN, suggesting that FMN may alleviate liver injury by regulating the gut microbiota (Fig. 5E). SCFA results showed no significant differences among the groups (Fig. 5G) and the detection technique was reliable (R>0.99, Fig. 5F).

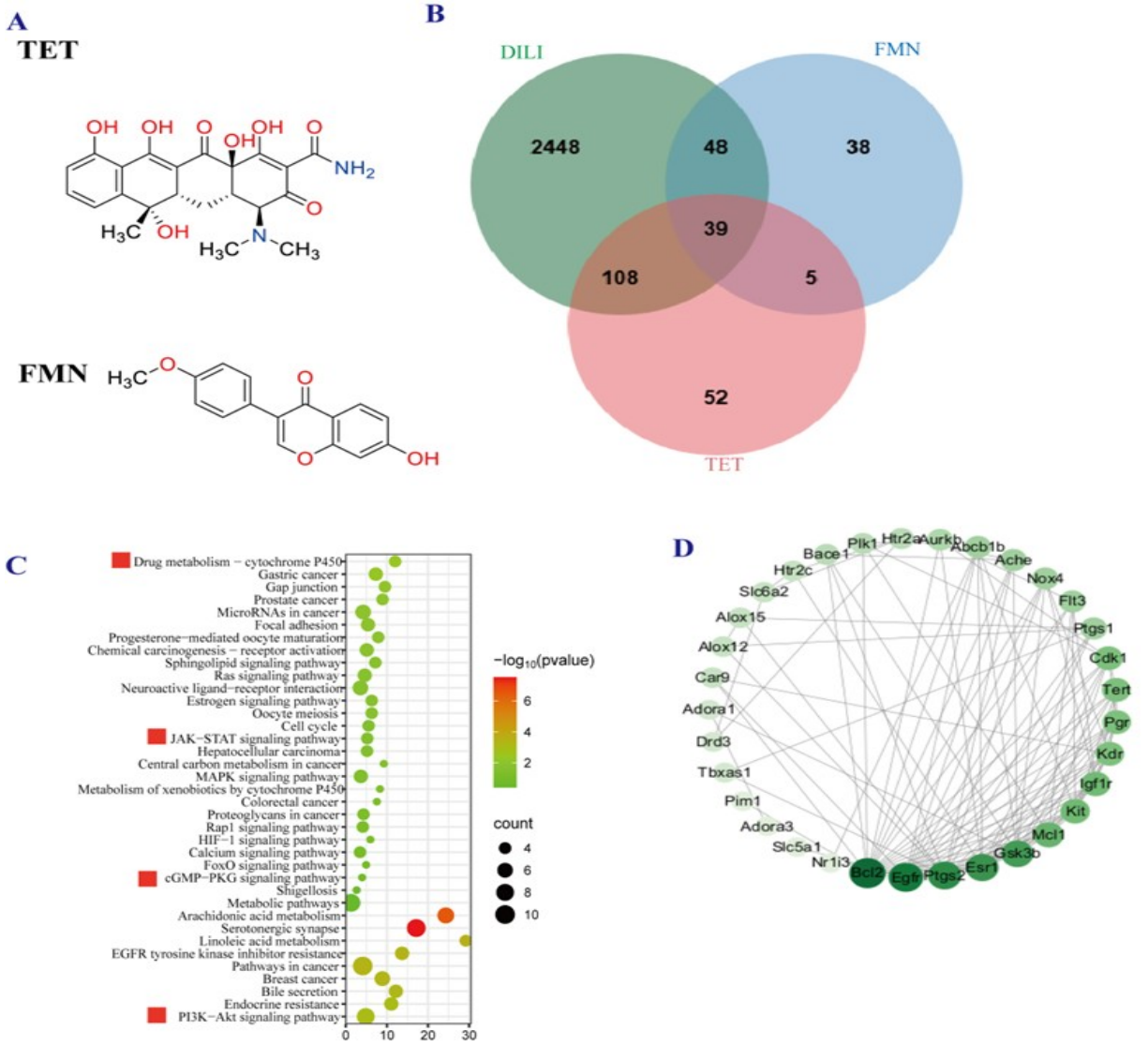

Fig. 1: Integrated network pharmacology analysis reveals core targets and pathways for FMN's protection against TET-induced injury. (A) 2D chemical structures of TET and FMN. (B) Venn diagram showing 39 common targets among DILI, TET, and FMN. (C) Top enriched KEGG pathways of the 39 common targets. (D) PPI network of common targets; node size and color indicate connectivity degree.

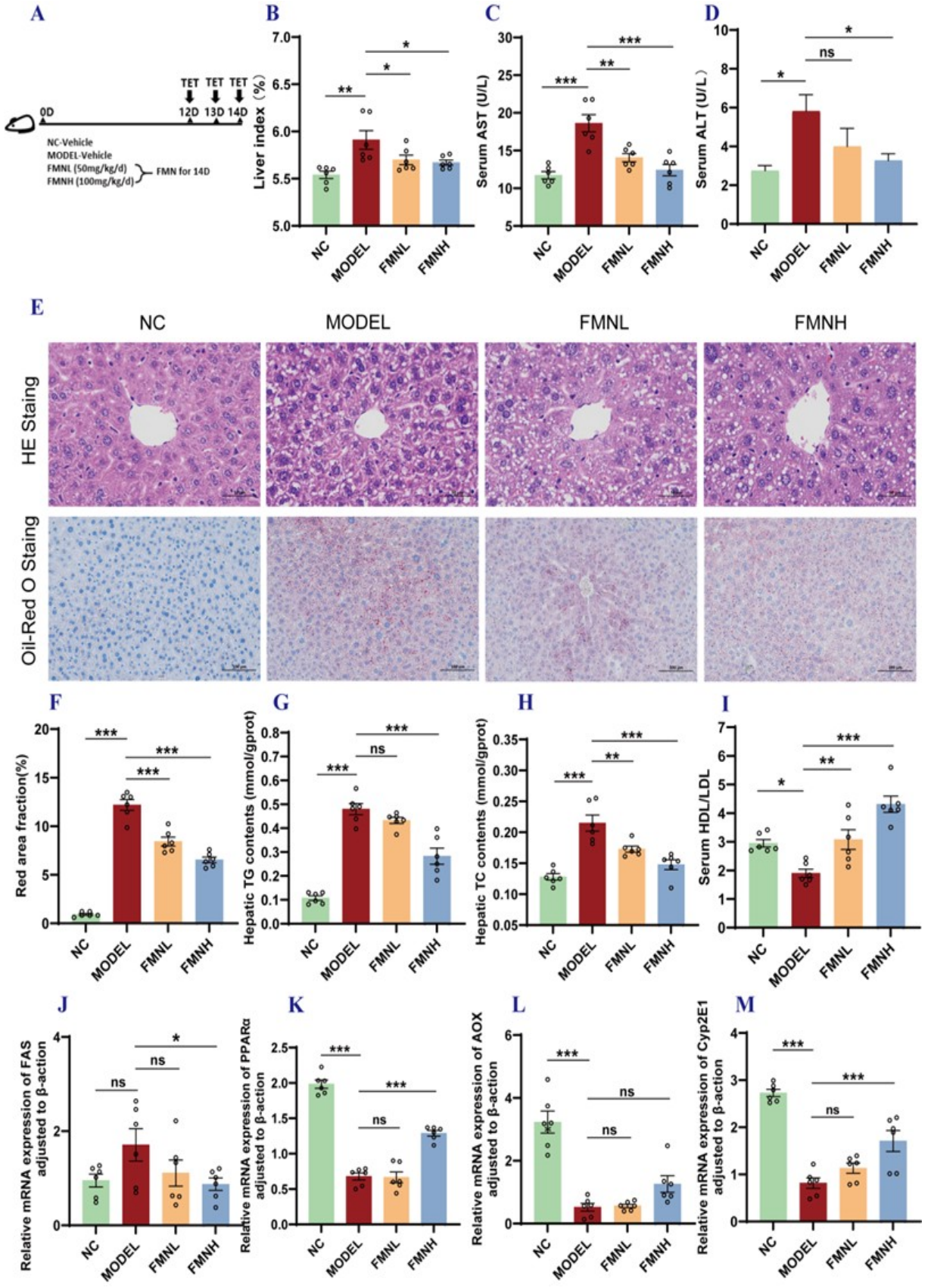

Fig. 2: FMN ameliorates TET-induced liver injury. (A) Experimental design. (B) Liver index. (C) Serum AST. (D) Serum ALT. © H&E and Oil Red O staining of liver. (F) Quantification of lipid droplet area. (G) Hepatic TG. (H) Hepatic TC. (I) Serum HDL/LDL ratio. (J) FAS mRNA expression (no significant change). (K-M) mRNA expression of β-oxidation genes: PPARα (K), AOX (L), CYP2E1 (M); all significantly downregulated (P<0.001). Note: ns: not significant, *P<0.05, **P<0.01 (two-tailed Student's t-test with FDR correction). (group size: n=6).

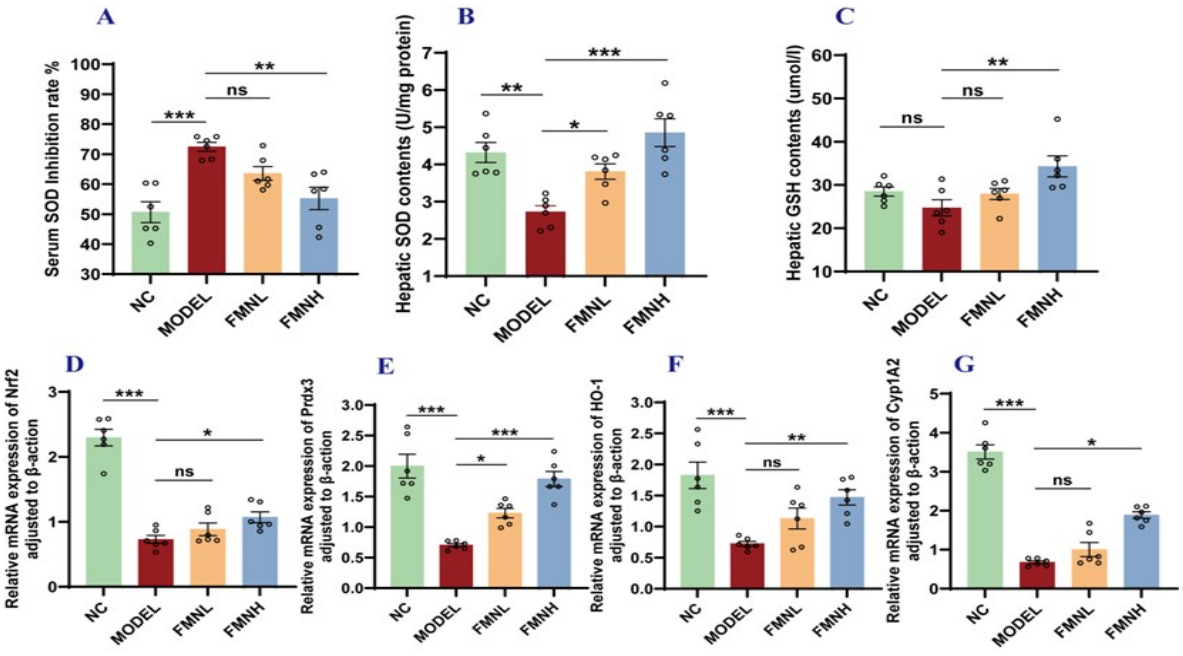

Fig. 3: FMN alleviates TET-induced lipid metabolism disorder. (A) Serum SOD inhibition rate. (B) Hepatic SOD. (C) Hepatic GSH. (D) Hepatic Cyp1a2 mRNA. © Hepatic *H0-1* mRNA. (F) Hepatic Prdx3 mRNA. (G) Hepatic *Nrf2* mRNA. Note: ns: not significant, *P<0.05, **P<0.01 (two-tailed Student's t-test with FDR correction).(group size: n=6). (group size: n=6).

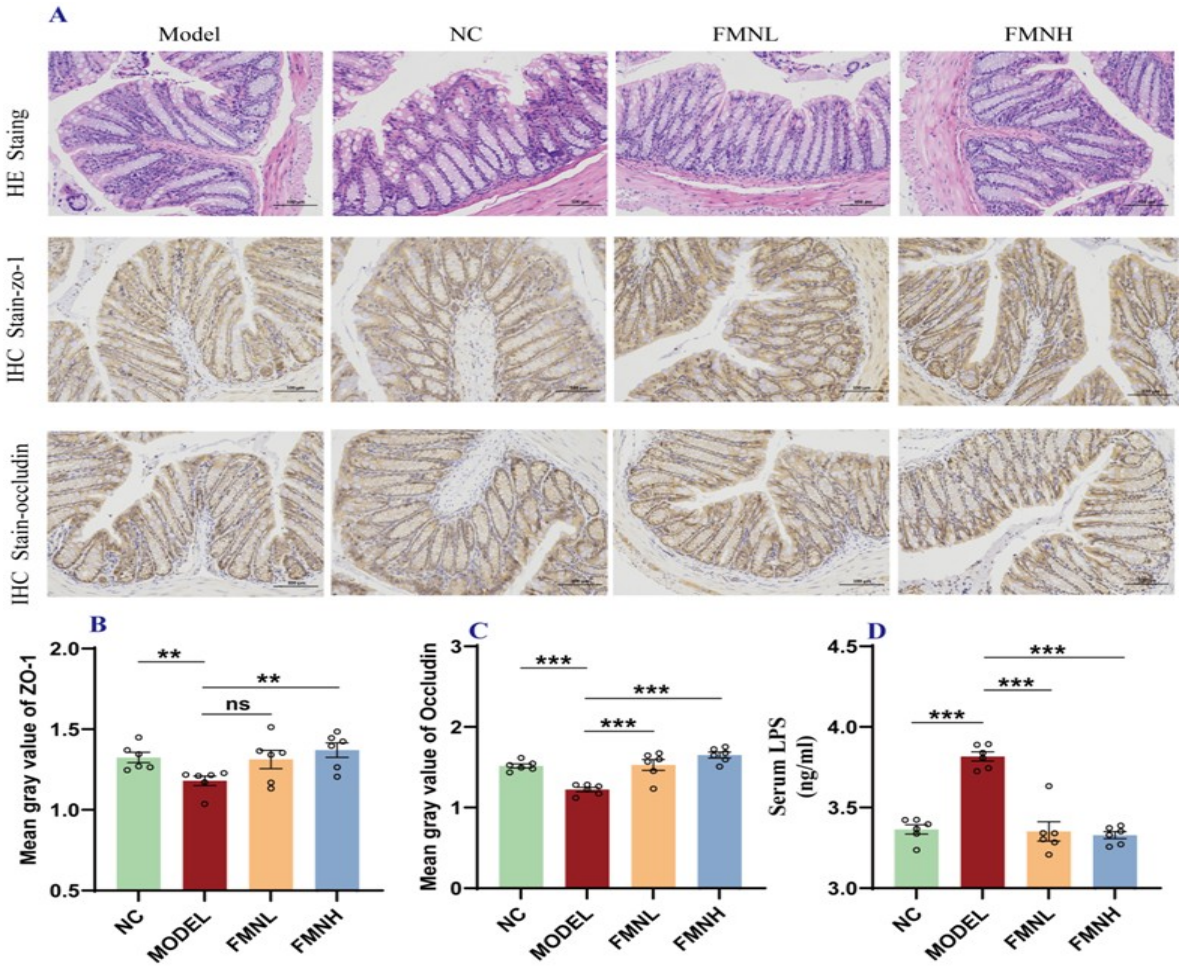

Fig. 4: FMN mitigates TET-induced intestinal barrier damage. (A) Representative images of H&E and IHC staining for *ZO-1* and 1157ccluding in colon tissue. (B) Quantification of *ZO-1* protein expression (IHC). (C) Quantification of 1157ccluding protein expression (IHC). (D) Serum LPS concentration. Note: ns: not significant, *P<0.05, **P<0.01 (two-tailed Student's t-test with FDR correction). (group size: n=6).

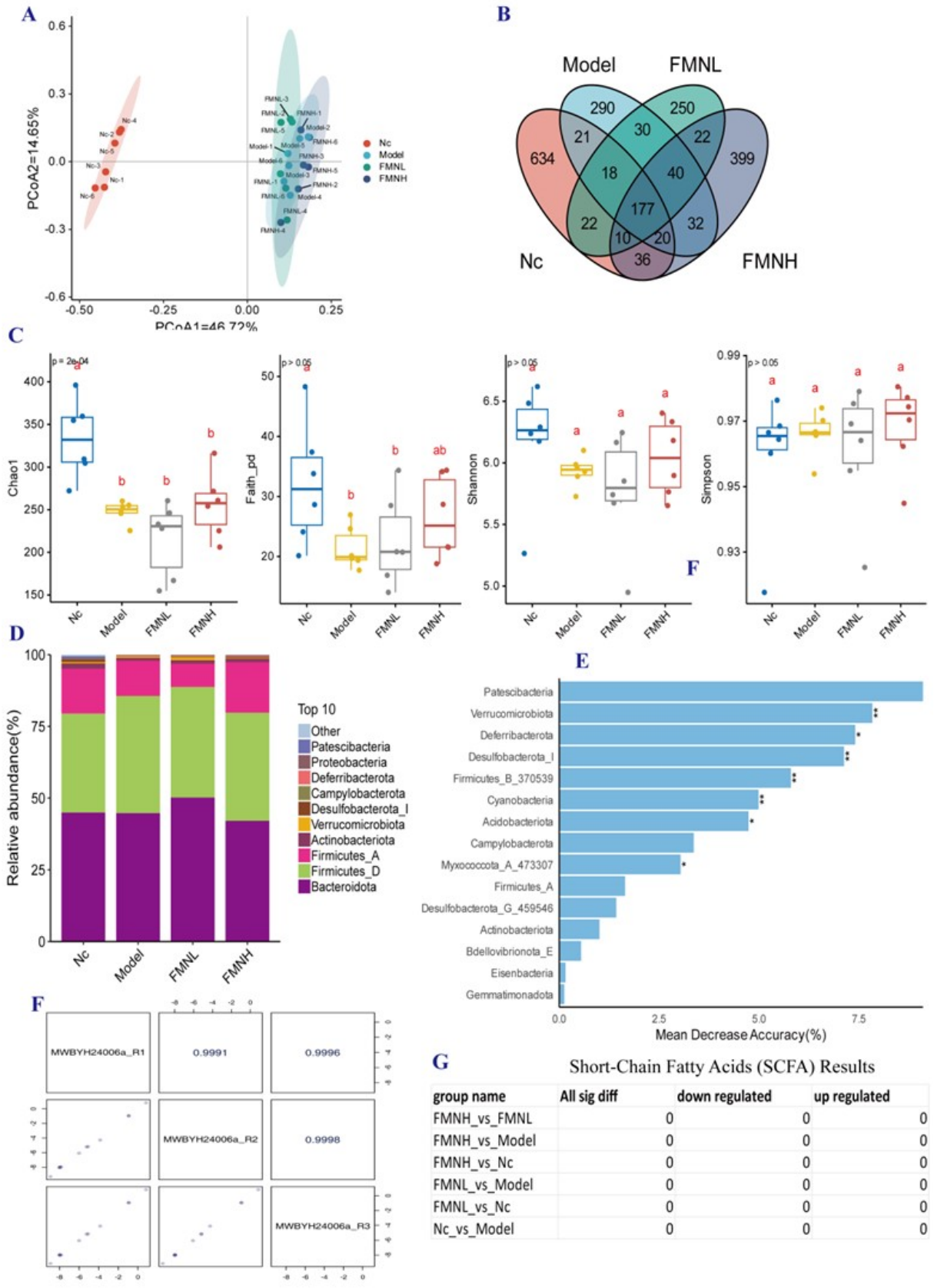

group name	All sig diff	down regulated	up regulated
FMNH_vs_FMNL	0	0	0
FMNH_vs_Model	0	0	0
FMNH_vs_Nc	0	0	0
FMNL_vs_Model	0	0	0
FMNL_vs_Nc	0	0	0
Nc_vs_Model	0	0	0

Fig. 5: FMNH modulates gut microbiota in TET-induced injury. (A) PcoA plot based on Bray-Curtis distance. (B) Venn diagram. (C) α-diversity analysis (Chao1, Faith's PD, Shannon and Simpson indices). (D) Phylum-level microbial composition. © LefSe analysis of phylum-level biomarkers. (F) Quality control of SCFA measurement. (G) Differential analysis of SCFAs. Note: ns: not significant, *P<0.05, **P<0.01 (two-tailed Student's t-test with FDR correction). (group size: n=6).

FMN regulates hepatic transcription: We performed transcriptome sequencing on the livers of each group. The results showed that compared to NC, MODEL exhibited 899 up- and 751 down-regulated genes (|FC|≥2, Fig. 6A). FMNH treatment reversed 169 of these genes (Fig. 6C), while FMNL affected 74 up- and 82 down-regulated genes (Fig. 6E). GO analysis showed enrichment in oxidoreductase/monooxygenase activity and iron binding (Fig. 6B, D, F). Key pathways among the top 20 KEGG terms included steroid hormone biosynthesis, xenobiotic metabolism by cytochrome P450, glutathione metabolism, and inflammatory mediator regulation of TRP channels (Fig. 7A, B, C), suggesting FMNH's role in metabolic detoxification and anti-inflammatory responses. Together, these results demonstrate that FMNH mitigates liver injury by coordinately regulating metabolic, inflammatory, and oxidative stress pathways. PPI network analysis identified key metabolic regulators, with FMNH treatment uniquely enriching cytochrome P450 genes (*CYP3A41B*, *CYP1A2*) and detoxification-related genes (GSTA3, DHCR7) (Fig. 7D&E), indicating enhanced hepatic detoxification capacity compared to FMNL.

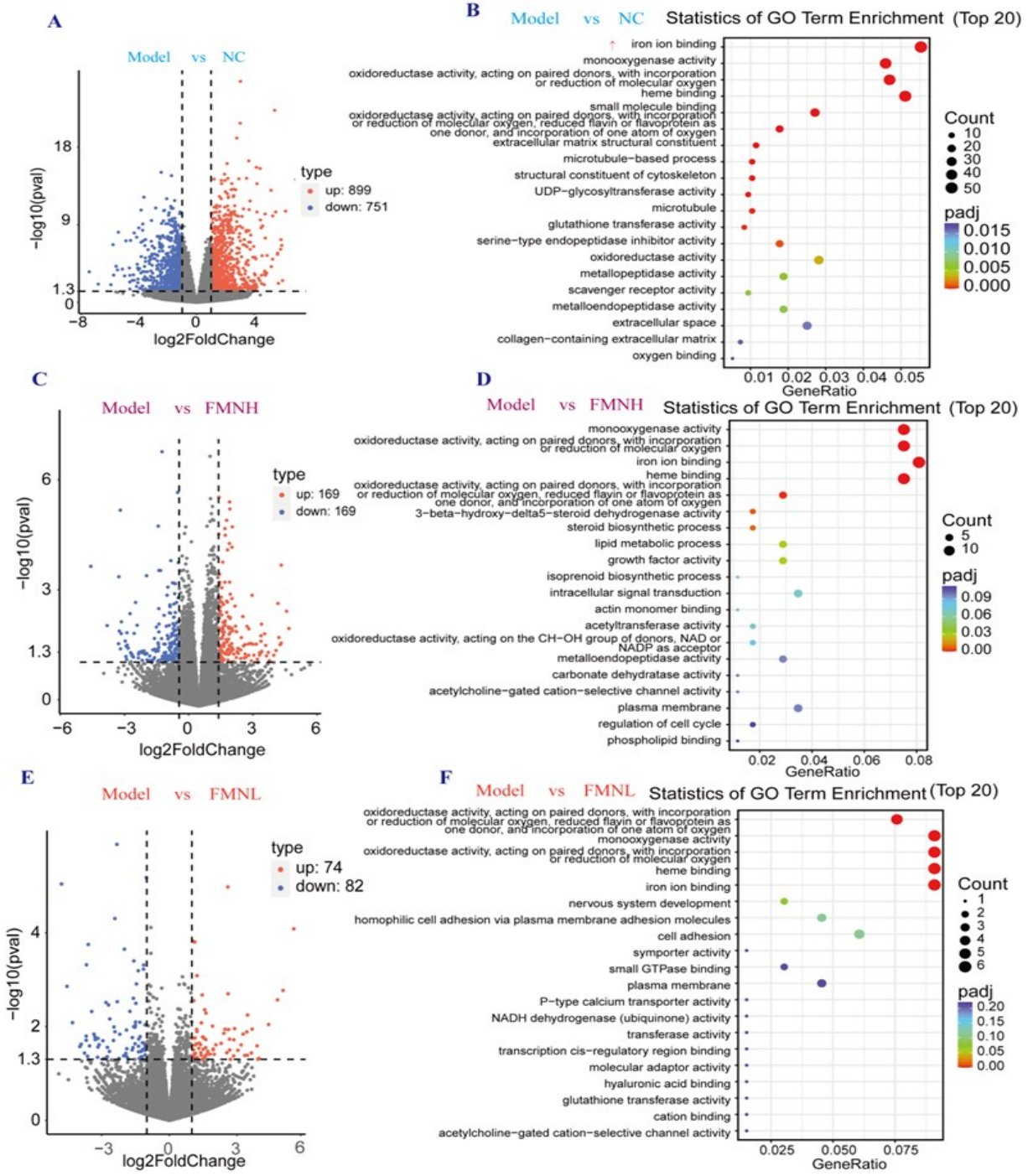

Fig. 6: FMNH regulates transcriptomic alterations in TET-induced liver injury. (A, C, E) Volcano plots of differentially expressed genes (DEGs). (B, D, F) GO enrichment analysis of top 20 DEGs. (group size: n=6).

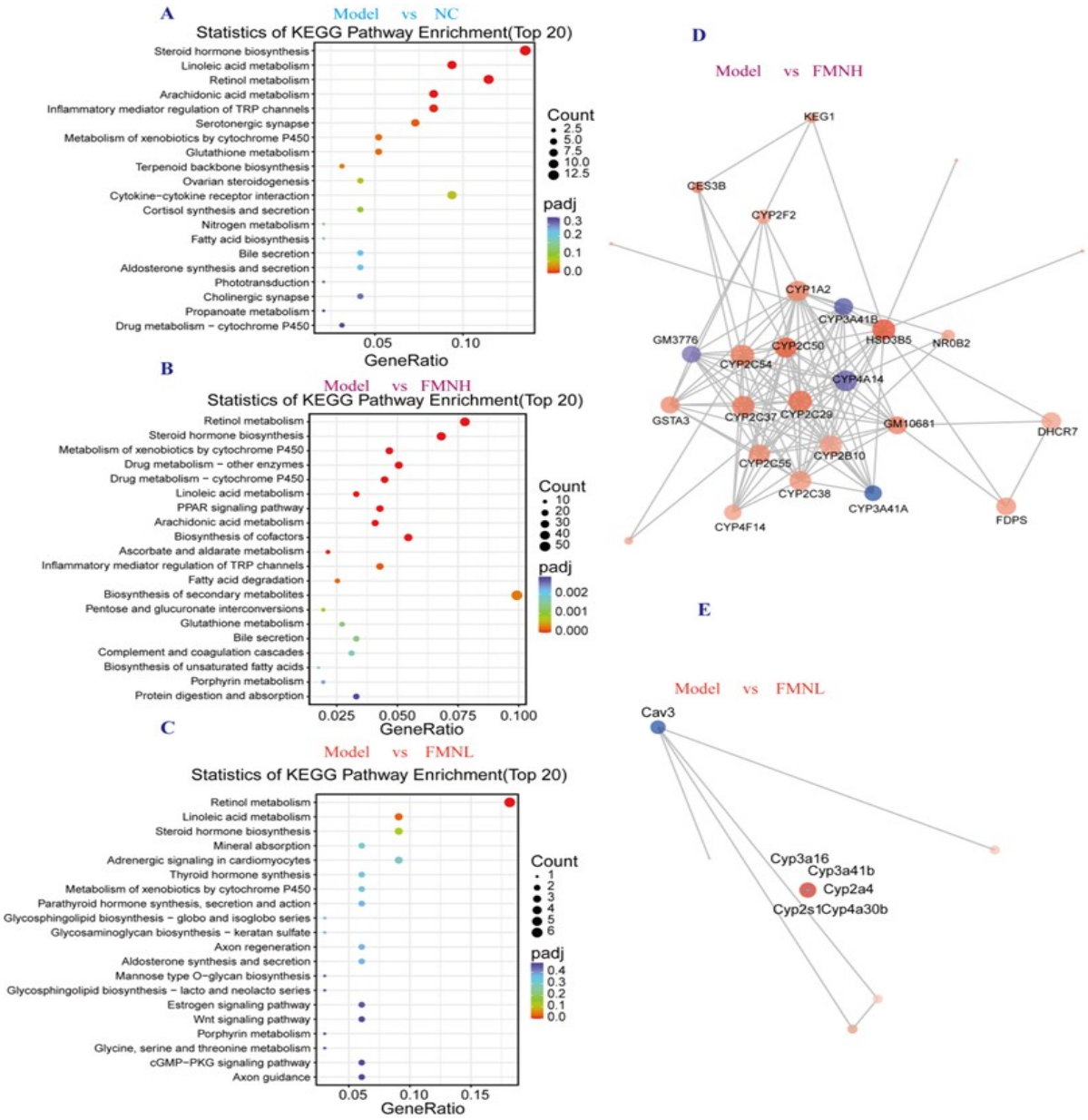

Fig. 7: Key pathways and genes regulated by FMNH in TET-induced liver injury. (A-C) KEGG pathway enrichment analysis (Top 20) of DEGs. (D-E) Protein-protein interaction (PPI) network analysis of DEGs.

FMN ameliorates TET-induced hepatic metabolic dysregulation: Hepatic metabolomic analysis revealed that TET exposure induced significant metabolic reprogramming, as shown by PCA (Fig. 8A) and OPLS-DA (Q^2 = 0.811; Fig. 9A), with clear separation between Model and NC groups. FMN treatment shifted the metabolic profile toward normalization. Using criteria of VIP≥1 and FC≥2 or ≤0.5, we identified that the Model group had 198 upregulated and 239 downregulated metabolites compared to NC (Fig. 8B). Relative to Model, FMNH treatment resulted in 140 upregulated and 67 downregulated metabolites (Fig. 8C), while FMNL led to 93 upregulated and 59 downregulated metabolites (Fig. 8D). KEGG enrichment analysis indicated that these differential metabolites were significantly enriched in the PI3K-AKT and cGMP-PKG signaling pathways (Fig. 8E-G). Specifically, TET depleted hepatoprotective lysophospholipids (LysoPC(14:1), LPE (18:1); Fig. 9B), accumulated xenobiotic metabolites (3'-azido-3'-deoxythymidine 5'-monophosphate; Fig. 9D) and disrupted bile acid conjugation (Fig. 9C). FMN dose-dependently reversed these perturbations (Fig. 9C-D), normalizing lysophospholipid profiles (LysoPC(14:1), LPC(17:1); Fig. 9B), reducing toxic xenobiotics, and restoring energy metabolites (GMP, acetyl-glycine; Fig. 9D). These findings demonstrate that FMN mitigates TET-induced hepatotoxicity by coordinating lipid homeostasis and detoxification pathways.

Integrated multi-omics analysis reveals gut microbiota-metabolite interactions and metabolic pathway dysregulation in TET-induced liver injury: To perform true multi-omics integration rather than presenting parallel datasets, we conducted

correlation-based network analysis linking gut microbiota, liver metabolites, and liver transcripts. Significant microbiota-liver metabolite associations were identified: Duboxiella positively correlated with 2-methylbutyric acid and *Limosilactobacillus* with decanoic acid (both P<0.01), while *Ligilactobacillus*, *Alistipes_A_871400, Butyricicoccus_A_77030*, *Sporofaciens and UBA11471* showed negative correlations with multiple short-chain fatty acids. These results demonstrate specific microbial contributions to host metabolite profiles, suggesting distinct functional roles in fatty acid metabolism in liver (Fig. 10A). Integrated analysis of differentially expressed genes and metabolites identified several significantly co-enriched KEGG pathways. The most prominent pathways included glutathione metabolism, fatty acid degradation and biosynthesis, and AMPK signaling pathway. Additional co-enriched pathways involved FoxO signaling, bile secretion, and glycosaminoglycan biosynthesis. These coordinated alterations suggest potential interplay between metabolic and transcriptional regulation in the Model group compared to FMNH (Fig. 10B). Our analysis identified significant positive correlations (P<0.05, R>0.5) between ferroptosis-related genes (*Fasn*, *Srebf1*, *Fdps*, *Cyp1a2*) and metabolites (Phe-Pro, Glu-Arg, Glycine), with Fasn showing the strongest associations (P<0.01). These metabolites also exhibited highly significant correlations with *Cyp2c37*, *Camp*, and *Pcsk9*, suggesting an interconnected regulatory network linking lipid metabolism, peptide homeostasis, and ferroptosis pathways. Notably, *Camp* demonstrated a strong association with Glu-Arg, while *Pcsk9* correlated significantly with Glycine, indicating potential crosstalk between metabolic and immune processes (Fig. 10C).

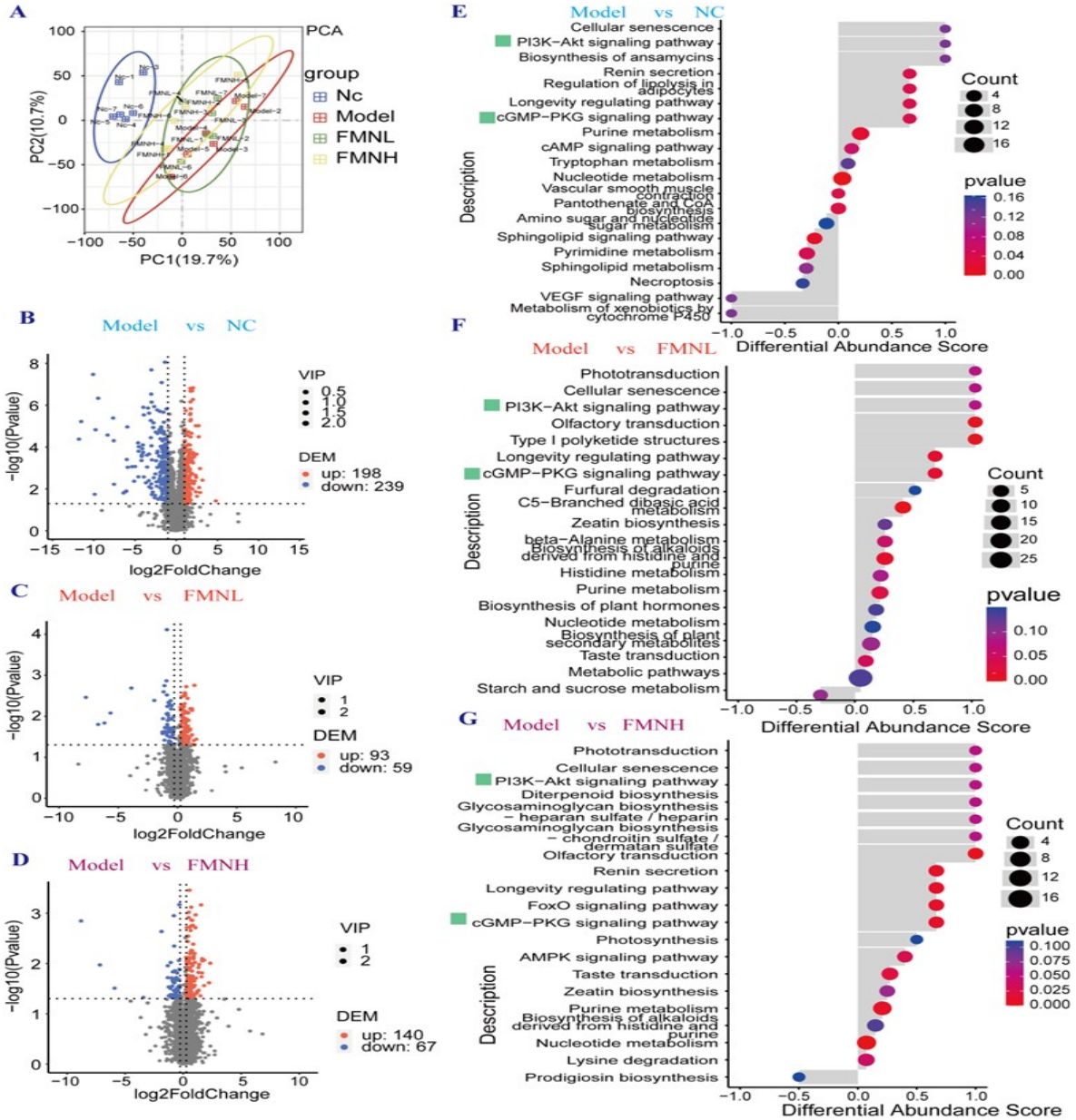

Fig. 8: Metabolomic landscape and pathway reprogramming by FMNH in TET-induced liver injury. (A) PCA plot. (B-D) Volcano plots of DEGs: (B) Model vs NC, (C) FMNL vs Model, (D) FMNH vs Model. (E-G) KEGG pathway enrichment analysis. (group size: n=6).

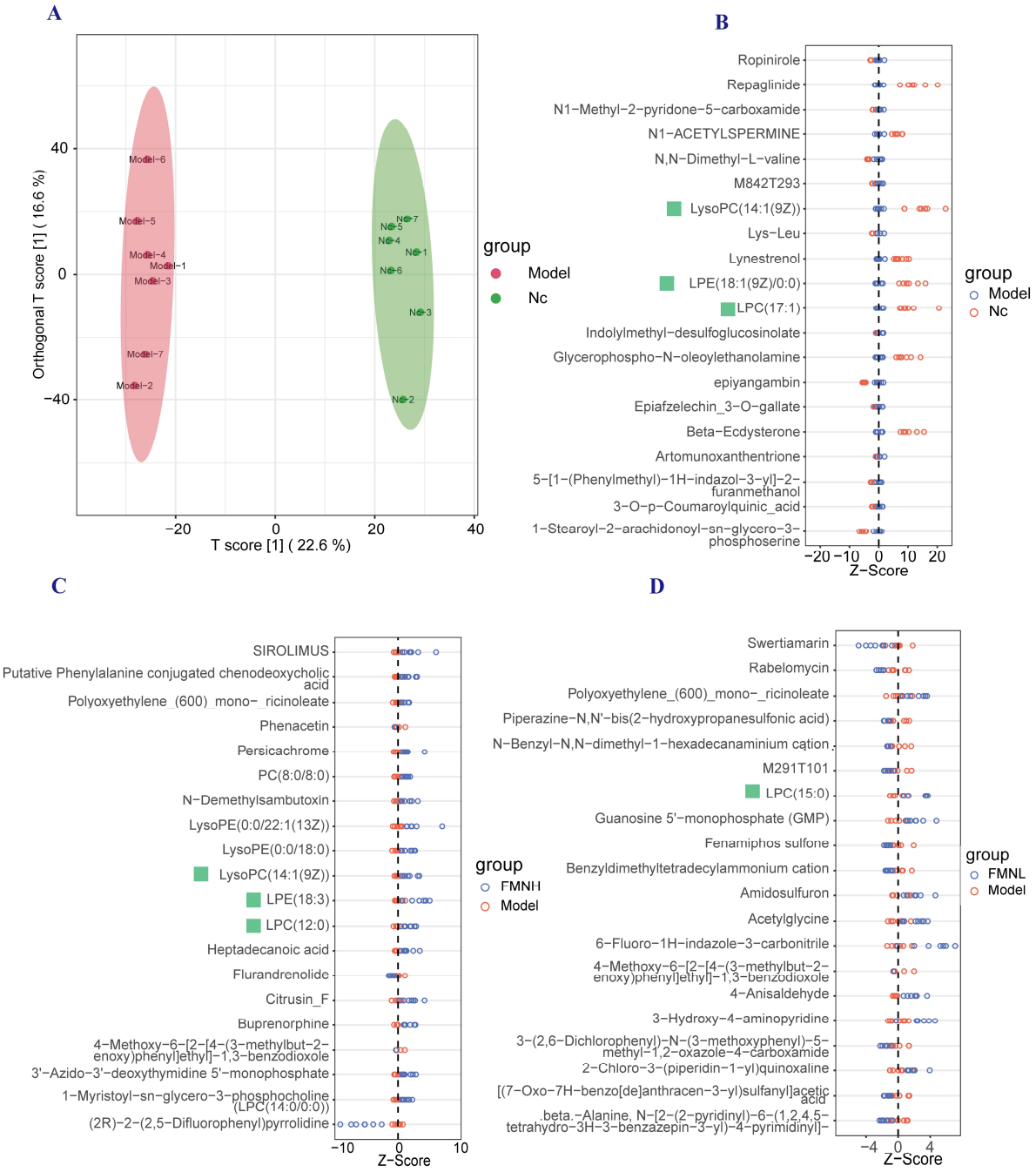

Fig. 9: Multivariate and differential metabolite analysis. (A) PCA score plot. (B-D) Stick plots of the differential metabolites between the compared groups (ordered by their Z-score value). (B) Model vs. NC group. (C) FMNH vs. Model group. (D) FMNL vs. Model group. (group size: n=6).

DISCUSSION

As the body's largest parenchymal organ, the liver executes essential metabolic, detoxification, and synthetic functions (Cheng *et al.*, 2021). In veterinary medicine, tetracycline antibiotics (oxytetracycline, doxycycline) are widely employed to treat respiratory and enteric infections in livestock and companion animals; however, their tetracycline antibiotics potential to induce subclinical hepatic dysfunction is often underestimated, potentially compromising animal growth performance and feed efficiency (Wu *et al.*, 2022; Liang *et al.*, 2024). While several multi-omics studies have described gut–liver axis changes during drug-induced liver injury, the specific mechanistic contribution of formononetin in tetracycline-induced hepatotoxicity has not been previously addressed. Tetracycline antibiotics, while clinically valuable, demonstrate significant hepatotoxicity that may progress to liver failure in susceptible individuals (Wang *et al.*, 2024a). Emerging evidence supports traditional medicine's role in NAFLD management (Lan *et al.*, 2022), particularly through early intervention in metabolic dysregulation (Zhang *et al.*, 2022).

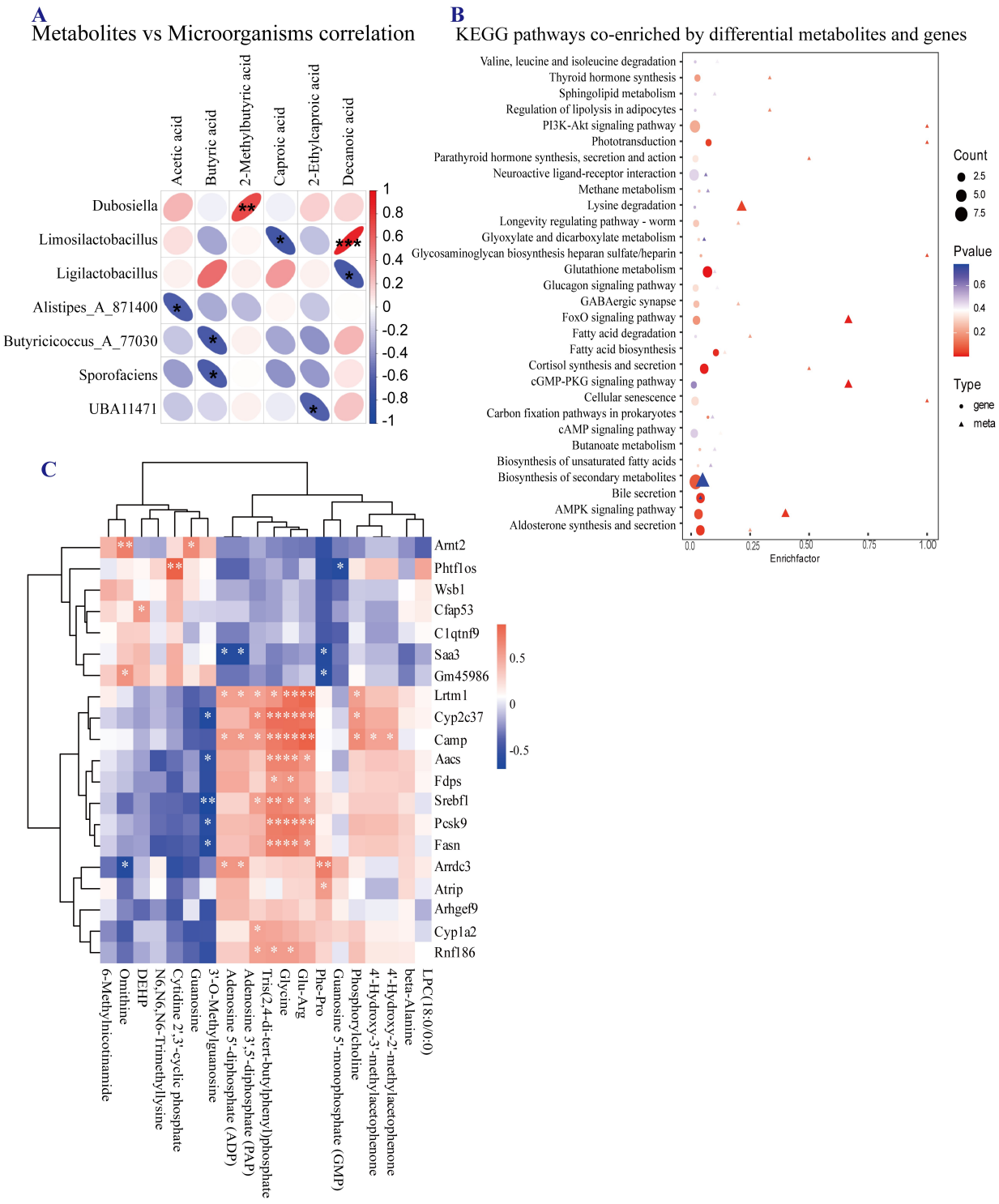

Fig. 10: Joint analysis. (A) Differential metabolites vs. differential microorganisms correlation. (B) KEGG pathways co-enriched by differential metabolites and differential genes. (C) Correlation analysis of ferroptosis-related genes and metabolites (group size: n=6).

Using network pharmacology, we identified 39 common targets among DILI, TET, and FMN, suggesting FMN modulates pathways involved in oxidative stress, inflammation, and cell survival. Enrichment of PI3K-Akt, cGMP-PKG, and JAK-STAT pathways aligns with their known roles in hepatocyte apoptosis and metabolic regulation (Zhang *et al.*, 2023; Wang *et al.*, 2024b; Shi *et al.*, 2025). Notably, these predicted pathways (PI3K-Akt, cGMP-PKG, JAK-STAT) were also enriched in our transcriptomic data (Fig. 8A-C), providing cross-validation between in silico predictions and experimental omics data. This consistency suggests that the network pharmacology predictions are reliable for generating hypotheses, although functional validation is still required. Hub genes such as Bcl2, Egfr, Ptgs2, and Mapk1 are involved in mitochondrial function and

oxidative stress (Zhao *et al.*, 2022; Zhu 2023; Liu *et al.*, 2025). Given the homology of these pathways across species, our *in-silico* findings support exploring FMN's hepatoprotective potential in veterinary contexts (Jiang *et al.*, 2025).

In a TET-induced mouse liver injury model, FMN intervention improved hepatic steatosis, as evidenced by reduced serum ALT, AST, and hepatic lipid accumulation (Zhai *et al.*, 2024). Mechanistically, TET inhibited fatty acid oxidation enzymes (*PPARα*, *AOX, CYP2E1*) in mitochondria, peroxisomes, and microsomes, while FMN treatment attenuated this inhibition, particularly restoring *PPARα* and *CYP2E1* expression, indicating that improvement in mitochondrial and microsomal function underlies its anti-steatotic effects(Zhao *et al.*, 2022). Additionally, TET-induced oxidative stress was evidenced by *NRF2* pathway suppression and reduced antioxidant components, whereas FMN upregulated Nrf2/HO-1-related transcripts and restored SOD/GSH levels at the protein level, indicating enhanced antioxidant capacity (Anandhan *et al.*, 2023; Panov, 2024; Sun *et al.*, 2025). FMN also reversed TET-induced downregulation of Prdx3, a mitochondrial peroxidase linked to ferroptosis. This is consistent with possible inhibition of ferroptosis, but direct evidence (e.g., GPX4, MDA, 4-HNE) is lacking (Oh *et al.*, 2022; Cui *et al.*, 2023). From a veterinary standpoint, reducing hepatic lipid accumulation is critical for preventing fatty liver in dairy cows and improving carcass quality in pigs, positioning FMN as a potential metabolic regulator in animal production (Du *et al.*, 2026).

The gut-liver axis plays a critical role in NAFLD progression, where microbial dysbiosis accelerates disease and intestinal barrier impairment allows LPS to reach the liver (Chu *et al.*, 2021; Hong *et al.*, 2021; Scarpellini *et al.*, 2024; Yibcharoenporn *et al.*, 2025). Our 16S rRNA sequencing revealed that TET exposure reduced gut microbial diversity, increased *Streptococcus* and *Erysipelotrichales*, and decreased beneficial taxa such as *Limosilactobacillus*, *Oscillospirales*, *Dubosiella*, and *Acutalibacteraceae*. FMN administration reversed these shifts and restored microbial equilibrium, demonstrating its capacity to maintain gut-liver axis homeostasis. In livestock, gut microbial equilibrium is linked to reduced subclinical infections and improved growth performance (Chen *et al.*, 2025), positioning FMN as a potential alternative to antibiotic growth promoters. Additionally, TET reduced intestinal barrier proteins ZO-1 and Occludin (Maali *et al.*, 2024) and elevated serum LPS levels, effects reversed by FMN, indicating FMN repairs the intestinal barrier and reduces endotoxin translocation.

Transcriptomic analysis showed that differentially expressed genes were involved in oxidoreductase activity, monooxygenase activity, and iron ion binding. Metabolomic analysis revealed that FMN modulated hepatic metabolites enriched in the PI3K-AKT pathway and cellular senescence. pAKT protects against stress-induced cell death (Shehu *et al.*, 2019), while oxidative stress can induce cellular senescence (Rodenak-Kladniew *et al.*, 2020), and slower senescence may increase tissue injury susceptibility (Huda *et al.*, 2019; Marin *et al.*, 2023). These findings suggest FMN repairs liver injury by enhancing antioxidant activity and inhibiting oxidative stress.

Integration of gut microbiota and liver metabolome data revealed that gut microbiota alterations were accompanied by altered levels of several microbiota-related fatty acids in the liver metabolome, including acetic acid, butyric acid, 2-methylbutyric acid, caproic acid, 2-ethylcaproic acid, and decanoic acid. Notably, fecal SCFA levels did not differ significantly among groups. Although speculative, this discrepancy may be attributable to methodological differences (targeted vs. untargeted detection) or temporal mismatches between cumulative fecal excretion and snapshot liver sampling ((Gao *et al.*, 2024; Kandalgaonkar *et al.*, 2024). Importantly, the lack of change in fecal SCFAs does not undermine the main conclusion that FMN protects against TET-induced liver injury via gut microbiota–liver crosstalk, as other microbial metabolites (e.g., bile acids, tryptophan derivatives) may play more prominent roles. Further studies are needed to identify the key mediators.

Integrated multi-omics analysis revealed coordinated dysregulation of lipid metabolism and redox pathways, with enrichment of glutathione metabolism and fatty acid degradation along with AMPK perturbations, suggesting a metabolic state favoring ferroptosis. Downregulation of GPX4, reduced GSH levels, and accumulation of peroxidation-prone PUFAs recapitulate ferroptosis signatures, which is consistent with a model in which gut dysbiosis contributes to metabolic disturbances that may promote ferroptotic hepatocyte death. Collectively, TET induces hepatotoxicity through oxidative stress and gut-derived endotoxin translocation, while FMN exerts multi-target protective effects by mitigating hepatic oxidative damage and intestinal barrier dysfunction. In summary, our findings suggest that FMN may confer protection through (1) regulation of PPARα/CYP2E1 to reduce lipid deposition, (2) activation of Nrf2/HO-1-related pathways to enhance antioxidant capacity and possibly inhibit ferroptosis, (3) improvement of gut microbiota diversity and intestinal barrier function to reduce LPS translocation, and (4) coordination of PI3K-AKT and glutathione metabolism to restore metabolic homeostasis.

Before concluding, several limitations of this study should be considered. The tetracycline exposure regimen consisted of three consecutive daily doses (150mg/kg/day), which models acute, overdose-induced hepatotoxicity. This model does not represent chronic, low-dose tetracycline exposure. However, acute liver injury following tetracycline or its derivative exposure is itself a clinically documented scenario (Silva *et al*., 2023; Wang *et al*., 2024a). Therefore, our findings should be interpreted within the context of acute tetracycline overdose rather than chronic exposure. Additionally, the sample size (n=6 per group) is relatively small for multi-omics integration, which may affect statistical power and reproducibility. This should be addressed in future studies with larger cohorts. Additionally, the network pharmacology predictions presented here are hypothesis-generating and require experimental validation (e.g., protein-level or functional assays) in future studies. Additionally, while our transcriptomic and biochemical data (SOD, GSH) support Nrf2/HO-1-mediated antioxidant effects, ferroptosis-related conclusions are based solely on Prdx3 mRNA changes and lack direct

protein-level validation (e.g., GPX4, MDA, 4-HNE). Functional ferroptosis assays are needed to confirm this mechanism. These findings position FMN as a promising multi-target hepatoprotective agent, though further research is needed to evaluate its clinical safety and long-term efficacy.

Conclusions: This study demonstrates that formononetin alleviates acute tetracycline-induced liver injury in mice by modulating the gut microbiota–liver axis. Integrated multi-omics analysis revealed that formononetin enhances gut microbial diversity, restores intestinal barrier integrity, and reduces LPS translocation. At the hepatic level, formononetin is associated with activation of the Nrf2/HO-1 pathway and possible inhibition of ferroptosis, along with regulation of PPARα/CYP2E1-mediated lipid metabolism. Although further validation (e.g., protein-level assays, larger animal models) is required, these findings provide a preliminary basis for evaluating formononetin as a potential hepatoprotective agent in veterinary settings in the future.

Acknowledgements: We acknowledge FigDraw (www.figdraw.com) for providing the tools to create the graphical abstract and the colleagues from the Institute of Traditional Chinese Veterinary Medicine of Nanjing Agricultural University. In addition, the authors extend their appreciation to the Deanship of Research and Graduate Studies at King Khalid University for funding this work through the Large Research Project under the large group grant number (R.G.P2/162/47), and Princess Nourah bint Abdulrahman University Researchers Supporting Project number (PNURSP2026R457),Princess Nourah bint Abdulrahman University, Riyadh,Saudi Arabia.

Conflict of interest: The authors declare that the research was conducted in the absence of any commercial or financial relationships that could be construed as a potential conflict of interest.

Funding: This study was financially supported by National Natural Science Foundation of China (Grant No. 82460796) (Ning Li), Yunnan Fundamental Research Projects (Grant No. 202301AS070081), Rural Vitalization Science and technology Project – Gejiu Cattle Industry Science and Technology Mission in Yunnan Province (Grant No. 202304BI090007) (Weijie Qu), Yunnan Joint International R&D Center of Veterinary Public Health (202403AP140033), the Deanship of Research and Graduate Studies at King Khalid University for funding this work through the Large Research Project under the large group grant number (R.G.P2/162/47), and Princess Nourah bint Abdulrahman University Researchers Supporting Project number (PNURSP2026R457),Princess Nourah bint Abdulrahman University, Riyadh,Saudi Arabia.

Authors contribution: XZ: Conceptualization, Writing - original draft, Formal analysis, Visualization; JS , XW : Methodology, Writing - original draft, Investigation, Data curation, Validation, Formal analysis, Visualization; EAA-S: Investigation, Data curation, Validation; LAA: Resources, Formal analysis, Visualization; JS , YY: Software, Validation, Resources; SC, WJ: Methodology, Investigation, Data curation, Formal analysis; YL, NW, YH: Project administration, Resources, Methodology, Investigation, Software, Validation; XG, JS: Writing - review & editing; WB: Supervision, Writing - review & editing; NL: Project administration, Conceptualization, Funding acquisition, Writing - review & editing; WQ: Supervision, Project administration, Conceptualization, Funding acquisition, Writing - review & editing.

Ethics approval and consent to participate: This process was conducted in compliance with the Yunnan Agricultural University Animal Ethics Committee (Permission code: 202405008, Date: 10 Sep. 2024).

Patient consent for publication: Not applicable.

Data available: All data supporting the findings of this study are publicly available. 16S rRNA sequencing data are deposited in NCBI BioProject under accession PRJNA1344615. Transcriptomics data are available in the OMIX database (China National Center for Bioinformation) under accession OMIX012352 (BioProject PRJCA048238). Untargeted metabolomics and targeted SCFA data are available in EMBL-EBI Metabolights under accessions MTBLS13138 and MTBLS13161, respectively.

REFERENCES

Anandhan A, Dodson M, Shakya A, *et al*., 2023. NRF2 controls iron homeostasis and ferroptosis through HERC2 and VAMP8. Science Advances 2023;9(5):eade9585.

Chen W, Ma Q, Li Y, *et al*., 2025. Butyrate supplementation improves intestinal health and growth performance in livestock: A review. Biomolecules 15(1):85.

Cheng ML, Nakib D, Perciani CT, *et al*., 2021. The immune niche of the liver. Clinical Science 135(20):2445-2466.

Cui S, Ghai A, Deng Y, *et al*., 2023. Identification of hyperoxidized PRDX3 as a ferroptosis marker reveals ferroptotic damage in chronic liver diseases. Molecular Cell 83(21):3931-3939.

Du X, Liu M, Lei L, *et al*., 2026. FOXA3 Alleviates lipid deposition in primary bovine hepatocytes by inhibiting SREBP1 and cell proliferation. Veterinary Sciences 13(2):157.

Gao Y, Yao Q, Meng L, *et al*., 2024. Double-side role of short chain fatty acids on host health via the gut-organ axes. Animal Nutrition (Zhongguo xu mu shou yi xue hui) 18:322-339.

Huda N, Liu G, Hong H, *et al*., 2019. Hepatic senescence, the good and the bad. World Journal of Gastroenterology 25(34):5069-5081.

Jiang C, Li Z, Seok S, *et al*., 2025. Systemic identification of functionally conserved long noncoding RNA metabolic regulators in human and mouse livers. Gastroenterology 169(4):676-690.

Kandalgaonkar MR, Kumar V and Vijay-Kumar M, 2024. Digestive dynamics: Unveiling interplay between the gut microbiota and the liver in macronutrient metabolism and hepatic metabolic health. Physiological Reports 12(12):e16114.

Kennedy L, Meadows V, Sybenga A, *et al*., 2021. Mast cells promote nonalcoholic fatty liver disease phenotypes and microvesicular steatosis in mice fed a western diet. Hepatology (Baltimore, Md.) 74(1):164-182.

Lan T, Jiang S, Zhang J, *et al*., 2022. Breviscapine alleviates NASH by inhibiting TGF-beta-activated kinase 1-dependent signaling. Hepatology 76(1):155-171.

Li C, Awasthi MK, Liu J, *et al*., 2024. Veterinary tetracycline residues: Environmental occurrence, ecotoxicity and degradation mechanism. Environmental Research 266:120417.

Liang Q, Xie C, Gebreselase HB, *et al*., 2024. Dynamic shifts in antibiotic residues and gut microbiome following tilmicosin administration to Silkie chickens. Animals14(23):3428.

Liao J, Xie X, Wang N, *et al*., 2024. Formononetin promotes fatty acid beta-oxidation to treat non-alcoholic steatohepatitis through SIRT1/PGC-1alpha/PPARalpha pathways. Phytomedicine 124:155285.

Liu C, He P, Qiao R, *et al*., 2025. Mechanistic study of *Lonicerae japonicae* Flos (Caprifoliaceae) in non-small cell lung cancer prevention and treatment through integrative pharmacology multi-machine learning, artificial intelligence, and *in-vitro* experiments. Journal of Ethnopharmacology 348:119832.

Liu L, Wang L, Pang K, *et al*., 2025. Source orientation, environmental fate, and risks of antibiotics in the surface water of the largest sediment-laden river. Environmental Pollution 126363.

Maali Y, Flores MM, Khedr O, *et al*., 2024. Two transcriptionally and functionally distinct waves of neutrophils during mouse acute liver injury. Hepatology Communications 8(7).

Marin I, Boix O, Garcia-Garijo A, *et al*., 2023. Cellular senescence is immunogenic and promotes antitumor immunity. Cancer Discovery 13(2):410-431.

Naudhani M, Thakur K, Ni ZJ, *et al*., 2021. Formononetin reshapes the gut microbiota, prevents progression of obesity and improves host metabolism. Food & Function 12(24):12303-12324.

Oh SJ, Ikeda M, Ide T, *et al*., 2022. Mitochondrial event as an ultimate step in ferroptosis. Cell Death Discovery 8(1):414.

Panov AV, 2024. The structure of the cardiac mitochondria respirasome is adapted for the β-Oxidation of Fatty acids. International Journal of Molecular Sciences 25(4).

Rodenak-Kladniew B, Castro A, Starkel P, *et al*., 2020. 1,8-Cineole promotes G0/G1 cell cycle arrest and oxidative stress-induced senescence in HepG2 cells and sensitizes cells to anti-senescence drugs. Life Sciences 243:117271.

Shao Q, Khawaja A, Nguyen MD, *et al*., 2025. T cell toxicity induced by tigecycline binding to the mitochondrial ribosome. Nature Communications 16(1):4080.

Shehu AI, Lu J, Wang P, *et al*., 2019. Pregnane X receptor activation potentiates ritonavir hepatotoxicity. Journal of Clinical Investigation 129(7):2898-2903.

Shi J, Chen J, Cheng C, *et al*., 2025. Systems pharmacology-based drug discovery and active mechanism of ganoderma lucidum triterpenoids for type 2 diabetes mellitus by integrating network pharmacology and molecular docking. Current Pharmaceutical Design 31(33):2666-2690.

Silva C, Merim S, Sevivas R, *et al*., 2023. Bismuth subcitrate, metronidazole and tetracycline-A rare cause of drug-induced liver injury. European Journal of Case Reports in Internal Medicine 10(12):004119.

Sun H, Liu T, Wang Z, *et al*., 2025. Role of Curcumin in chronic liver diseases: A comprehensive review. Drug Design Development and Therapy 19:3395-3406.

Tay KC, Tan LT, Chan CK, *et al*., 2019. Formononetin: A review of its anticancer potentials and mechanisms. Frontiers in Pharmacology 10:820.

Tóth G, Jones A, Montanarella L, 2013. The LUCAS topsoil database and derived information on the regional variability of cropland topsoil properties in the European Union. Environmental Monitoring and Assessment 185(9):7409-25.

Vitale G, Mattiaccio A, Conti A, *et al*., 2023. Molecular and clinical links between drug-induced cholestasis and familial intrahepatic cholestasis. International Journal of Molecular Sciences 24(6):24065823.

Wang K, Yin J, Chen J, *et al*., 2024a. Inhibition of inflammation by berberine: Molecular mechanism and network pharmacology analysis. Phytomedicine 128:155258.

Wang R, Li Y, Xia X, *et al*., 2024b. Severe liver injury induced by minocycline in hepatitis B patient: a Case Report. Frontiers in Pharmacology 15:1516217.

Wang Y, Zhao H, Li X, *et al*., 2019. Formononetin alleviates hepatic steatosis by facilitating TFEB-mediated lysosome biogenesis and lipophagy. Journal of Nutritional Biochemistry 73:108214.

Wei C, Liu Y, Jiang A, *et al*., 2022. A pharmacovigilance study of the association between tetracyclines and hepatotoxicity based on food and drug administration adverse event reporting system data. International Journal of Clinical Pharmacy 44(3):709-716.

Wu G, Sun L, Xu J, *et al*., 2022. Efficient degradation of tetracycline antibiotics by engineered myoglobin with high peroxidase activity. Molecules (Basel, Switzerland) 27(24):8660.

Yang SE, Lien JC, Tsai CW, *et al*., 2022. Therapeutic potential and mechanisms of novel simple o-substituted isoflavones against cerebral ischemia reperfusion. International Journal of Molecular Sciences 23(18):231810394.

Yibcharoenporn C, Muanprasat C, Moonwiriyakit A, *et al*., 2025. AMPK in intestinal health and disease: A multifaceted therapeutic target for metabolic and inflammatory disorders. Drug Design Development and Therapy 19:3029-3058.

Zhai Z, Yang Y, Chen S, *et al*., 2024. Long-term exposure to polystyrene microspheres and high-fat diet-induced obesity in mice: Evaluating a role for microbiota dysbiosis. Environmental Health Perspectives 132(9):97002.

Zhang P, Zhang D, Zhou W, *et al*., 2023. Network pharmacology: towards the artificial intelligence-based precision traditional Chinese medicine. Briefings in Bioinformatics 25(1): 518.

Zhang XL, Wang TY, Targher G, *et al*., 2022. Lifestyle interventions for non-obese patients both with, and at risk, of non-alcoholic fatty liver disease. Diabetes & Metabolism Journal 46(3):391-401.

Zhang YZ, Zhang J, Tan L, *et al*., 2018. Preparation and evaluation of temperature and magnetic dual-responsive molecularly imprinted polymers for the specific enrichment of formononetin. Journal of Separation Science 41(15):3060-3068.

Zhao Q, Bai J, Chen Y, *et al*., 2022. An optimized herbal combination for the treatment of liver fibrosis: Hub genes, bioactive ingredients, and molecular mechanisms. Journal of Ethnopharmacology 297:115567.

Zhao T, Yu Z, Zhou L, *et al*., 2022. Regulating Nrf2-GPx4 axis by bicyclol can prevent ferroptosis in carbon tetrachloride-induced acute liver injury in mice. Cell Death Discovery 8(1):380.

Zhu Z, Jiang H, 2023. Identification of oxidative stress-related biomarkers associated with the development of acute-on-chronic liver failure using bioinformatics. Scientific Reports 13(1):17073.